University of Thi-Qar Journal

ISSN (print): 2706- 6908, ISSN (online): 2706-6894

Vol.21 No.2 june 2026

A comparative study of noise-affected magnetic resonance image segmentation using traditional and robust Otsu algorithms with region of interest determination

Fahad Hussein Enad[1], Asmaa Ghalib Jaber[2]

[1]Department of Studies and Planning, University of Dhi Qar, Al-Nasiriyah, Dhi Qar, Iraq

https://orcid.org/0000-0002-0209-9206

[2]Department of Statistics, College of Administration and Economics, University of Baghdad, Al-Waziriya, Baghdad, Iraq

{fahadh@utq.edu.iq , Drasmaa.ghalib@coadec . uobaghdad@edu.iq }

Abstract

Medical image segmentation systems face significant challenges when processing magnetic resonance imaging (MRI) images of brain tumors, especially given the low contrast and presence of noise, which affects the accuracy of tumor region identification. This study aims to compare the performance of the classical Otsu algorithm with Robust Otsu in segmenting noise-affected images, focusing on threshold stability and separation accuracy. The two methods were applied to MRI images from the BraTS 2023 database, which included 23 clinical cases, using the original images and corrupted copies with different noise levels (0, 0.03, 0.06, 0.1). The experiments were performed using MATLAB 2024, and the evaluation was based on quantitative indicators including Dice, IoU, MSE, and Accuracy. The results showed that the performance of classical Otsu deteriorated with increasing noise, while Robust Otsu maintained more stable performance, achieving higher Dice values, a significant decrease in MSE, and improved accuracy across all noise levels. These results confirm that developing the Otsu algorithm to be more robust is a practical, simple, and effective solution for improving the segmentation of blurred medical images without the need for high computational complexity or resource-intensive deep learning models.

Keywords: Medical Image Segmentation, Brain MRI, Otsu Thresholding, Robust Thresholding, Noise Robust Segmentation

University of Thi-Qar Journal
ISSN (print): 2706- 6908, ISSN (online): 2706-6894
Vol.21 No.2 june 2026

1-Introduction:

Image segmentation is one of the fundamental pillars of digital image processing, as it aims to divide the image into homogeneous regions that facilitate its analysis and the extraction of information from it, which directly reflects on the efficiency of medical and engineering applications and remote sensing. Segmentation is increasingly important in medical images, especially magnetic resonance imaging (MRI) of brain tumours, because the accuracy of tumour boundary determination and isolation is linked to the quality of diagnosis and treatment plans. Capelle et al. (2000) addressed this issue through a two-stage automatic segmentation approach to isolate the brain and then segment it internally to detect the tumour, noting that the limited number of cases and the lack of extensive comparisons may restrict the generalisation of the results [1]. Ruan et al. (2002) also pointed out that the complexity of brain structure and the effect of partial volume increase the difficulty of separating tissues, noting that segmentation performance declines with increasing noise levels, confirming that noise remains a critical factor in segmentation success. Noise of various types, such as Gaussian noise and speckle noise, is one of the most significant obstacles to segmentation, as it weakens edges and distorts the statistical distribution of intensity values, particularly by changing the shape of the histogram and reducing the separation between categories[2]. Gonzalez and Woods (2008) showed that any distortion in the histogram caused by noise directly affects the accuracy of global thresholding methods, as they rely on the grey statistics of the image. This problem is even more pronounced in thresholding methods, which rely directly on the characteristics of the statistical distribution. Among thresholding methods [3], the Otsu algorithm (1979) stands out as one of the most popular unsupervised methods, as it relies on maximising the contrast between categories or minimising the contrast within them. It has proven effective in images with clear grey distribution, but its sensitivity to frequency distribution distortion under the influence of noise makes its performance less stable in noisy images, as noted by a number of researchers in the context of evaluating Otsu's performance under non-ideal conditions[4]. Sezgin and Sankur (2004) confirmed in their comparative study of thresholding methods that Otsu's performance deteriorates

significantly in the presence of high noise or interference between categories, highlighting the need for developments that make thresholding more robust. Because of this shortcoming, research has focused on developing 'robust' versions of Otsu to improve thresholding decisions in the presence of noise, rather than relying solely on the classic Otsu[5]. Buenestado and Acho (2017) proposed a method that combines statistical confidence intervals and the Otsu algorithm to improve segmentation, especially in the presence of speckle noise. The results showed superiority over traditional Otsu by reducing the impact of noise and improving separation accuracy, using evaluation metrics such as the Jaccard index[6]. A study by Jaber et al. (2021) supported this trend through a two-stage approach that uses confidence intervals in pre-processing to improve the handling of noise-affected values, followed by thresholding. The results showed improved segmentation quality in both original images and those with speckle noise, indicating that introducing a statistical perspective into the threshold decision can increase stability and accuracy in noisy environments[7]. These results are consistent with what Xu et al. (2024) pointed out in their recent review of medical image segmentation techniques, where they showed that traditional methods such as thresholding are still characterised by simplicity and computational efficiency, but require further improvements to deal with noise and weak edges, making the development of robust versions of Otsu a justified and valuable research direction[8]. Based on this, the research problem is the noticeable decline in the performance of classical Otsu when applied to images affected by different levels of noise due to the distortion of the histogram and the weak contrast between categories, resulting in errors in threshold determination and failure to isolate areas of interest. There is also a continuing need for a clear systematic comparison between the classic Otsu and robust Otsu algorithms under various noise scenarios and using standardised quantitative measures. Therefore, this research aims to conduct a comparative study between the classical Otsu algorithm and a number of robust Otsu algorithms for segmenting noise-affected images, by analysing stability and accuracy under different noise conditions, and evaluating the results using quantitative indicators such as Dice, IoU, MSE, and Accuracy, in addition to visual evaluation, thereby contributing to determining the most

University of Thi-Qar Journal
ISSN (print): 2706- 6908, ISSN (online): 2706-6894
Vol.21 No.2 june 2026

appropriate method for segmenting noisy images within simple, fast, and practical solutions.

2-Theoretical aspect

2-1.Otsu's method

Otsu's method is a threshold-based image segmentation method used to convert a grayscale image into a binary image by classifying pixels into two categories: background and foreground. This method relies on analyzing the image's histogram and is effective when there is a binary distribution of intensities. The Otsu method is based on a statistical principle that aims to select the optimal threshold that minimizes the contrast within categories or, equivalently, maximizes the contrast between categories[4]. This is done by examining all possible threshold values within the range of light intensities, where for each threshold value, the probabilities of the two categories and the associated arithmetic means and variances are calculated. Intra-class variance is defined as follows[9][10] .

$$S_w^2(x) = w_1(x)s_1^2(x) + w_2(x)s_2^2(x) \quad (1)$$

Whereas:w_1: Probability associated with category 1,، :w_2:Probability associated with category 2,، x:Threshold separating the probabilities of the two categories, s_1^2:Variance associated with category 1,، s_2^2:Variance associated with category 2

The probability formula for categories based on L categories in the frequency distribution is presented as follows

$$w_1(x) = \sum_{j=0}^{x-1} \rho(j) \quad (2)$$

$$w_2(x) = \sum_{j=x}^{L-1} \rho(j) \quad (3)$$

Where $\rho(j)$ represents the natural probability of intensity level j, with the sum of probabilities property satisfied,j: gray level index,L: total number of gray levels (usually 256),x: threshold value, $w_1(x)$: probability of class 1 (background), $w_2(x)$: probability of class 2 (foreground).It should be noted that the threshold x represents the

University of Thi-Qar Journal
ISSN (print): 2706- 6908, ISSN (online): 2706-6894
Vol.21 No.2 june 2026

first gray level of the second class; therefore, the first class includes intensity levels from 0 to x-1, while the second class includes levels from x to L-1

$$w_1(x) + w_2(x) = 1 \quad (4)$$

Arithmetic mean equations for categories The arithmetic mean equations for each category are presented as follows

$$\mu_1(x) = \sum_{j=0}^{x-1} \frac{j\rho(j)}{w_1(x)} \quad (5)$$

$$\mu_2(x) = \sum_{j=x}^{L-1} \frac{j\rho(j)}{w_2(x)} \quad (6)$$

Where $\mu_1(x)$, $\mu_2(x)$ represents the arithmetic means related to the first and second categories, respectively, whileμ_T represents the total arithmetic mean.

$$\mu_T = \sum_{j=0}^{L-1} j\rho(j) \quad (7)$$

μ_T: total mean of the image.

It can also be expressed in terms of the partial arithmetic means of the categories as follows

$$\mu_T = w_1(x)\mu_1(x) + w_2(x)\mu_2(x) \quad (8)$$

Total variance is defined as the sum of variance within categories and variance between categories. For a given sample, total variance is calculated by summing the weighted squared distances between the overall mean and the means for each category. The variance for each category is calculated using the two equations provided for this purpose[11][12].

$$s_1^2(x) = \frac{\sum_{j=0}^{x-1}[j-\mu_1(x)]^2\,\rho(j)}{w_1(x)} \quad (9)$$

$$s_2^2(x) = \frac{\sum_{j=x}^{L-1}[j-\mu_2(x)]^2\,\rho(j)}{w_2(x)} \quad (10)$$

Where $s_1^2(x)$, $s_2^2(x)$ expresses the variance within the first category and the second category, respectively. The total variance is expressed by the following equations

University of Thi-Qar Journal

ISSN (print): 2706- 6908, ISSN (online): 2706-6894

Vol.21 No.2 june 2026

$$s^2 = s_w^2(x) + w_1(x)w_2(x)[\mu_1(x) - \mu_2(x)]^2 \quad (11)$$

$$s^2 = s_w^2(x) + s_b^2(x) \quad (12)$$

Where: s^2: is the total variance, $s_w^2(x)$*:* represents the variance within the category, $s_b^2(x)$: represents the variance between categories

The total variance is not affected by the variables x and constants, which means that rearranging the equations does not affect the calculated values. According to Otsu's method, reducing the variance within categories is equivalent to maximizing the variance between categories.

Steps of the Otsu method

Step 1: Calculate the histogram of the grayscale image and determine the probabilities of the intensity levels for each level.

Step 2: Initialize the initial values for the probabilities of the categories $w_j(x)$ and the corresponding $\mu_j(x)$ class means

Step 3: Perform iterations on all possible threshold values x within the image's intensity range, where the values of 8-bit magnetic resonance images fall within the range [0:255].

Step 4: Update the category probability values and partial arithmetic means for each threshold.

Step 5: Calculate the variance between categories $S_b^2(x)$ for each threshold value.

Step 6: Determine the optimal threshold that achieves the greatest value of variance between classes. $S_b^2(x)$

Step 7: Convert the grayscale image to a binary image using the determined optimal

University of Thi-Qar Journal

ISSN (print): 2706- 6908, ISSN (online): 2706-6894

Vol.21 No.2 june 2026

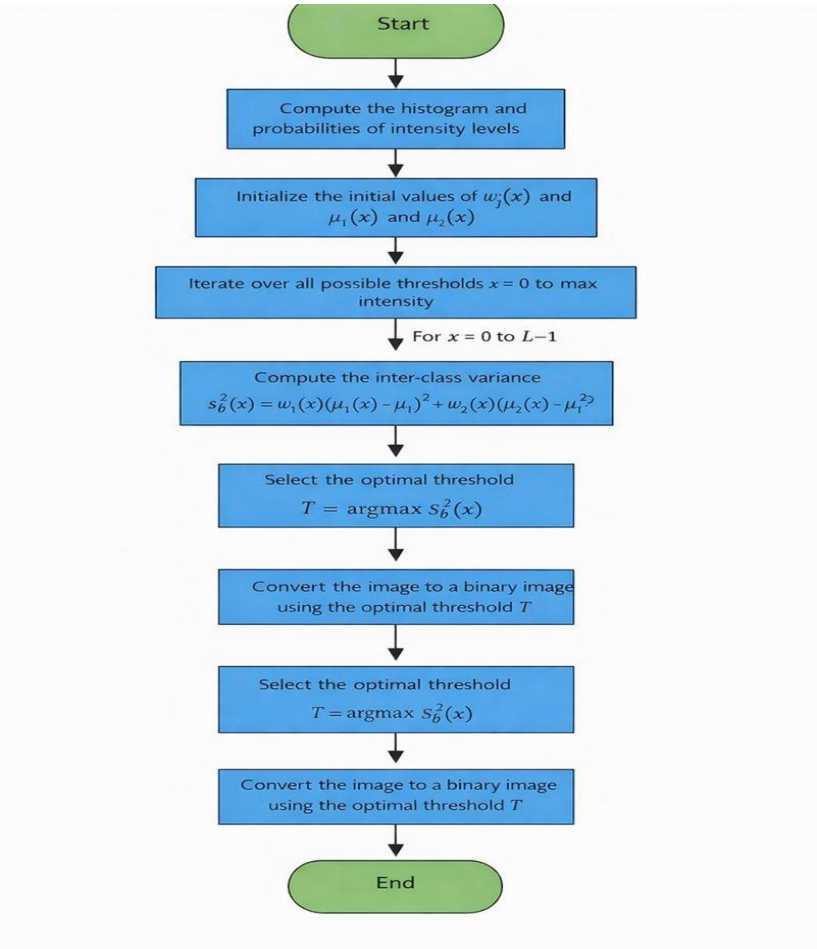

Figure 2.1: shows the flowchart of the Otsu method.

2-2.The proposed robust method Robust Otsu Thresholding

Magnetic resonance imaging (MRI) images often contain noise and outliers that directly affect threshold estimation in traditional statistical segmentation methods, such as the classic Otsu method based on arithmetic mean and variance. These measures are sensitive to outliers, which can lead to suboptimal threshold selection, especially in images with low contrast or asymmetric distributions. Based on this, the proposed robust method (Robust Otsu – ROtsu) was developed based on the median and median absolute deviation (MAD) as robust measures of central tendency and dispersion within categories, due to their high resistance to noise and histogram distortions, which is reflected in improved segmentation accuracy. The proposed method relies on analyzing

University of Thi-Qar Journal
ISSN (print): 2706- 6908, ISSN (online): 2706-6894
Vol.21 No.2 june 2026

the histogram of a grayscale image with L levels of illumination, so that the sum of the probability distribution satisfies the condition[13][14][15][16][17]:

$$\sum_{j=0}^{L-1} \rho(j) = 1 \quad (13)$$

Where: L: the number of brightness levels in the image (usually 256 for an 8-bit image), :j brightness level (gray pixel), where: $0 \leq j \leq L-1$. When a certain threshold x is applied, the pixels are divided into two categories: background and target (tumor), and the probability of each category is given by the formula[18]

$$w_1(x) = \sum_{j=0}^{x-1} \rho(j) \, , w_2(x) = \sum_{j=x}^{L-1} \rho(j) \quad (14)$$

Where :$\rho(j)$: The statistical probability of level j in the frequency distribution, subject to the condition:

$$w_1(x) + w_2(x) = 1 \quad (15)$$

Where: $w_1(x)$:probability of the first category (background), $w_2(x)$:probability of the second category (target/tumor)

To compensate for the sensitivity of the arithmetic mean to outliers, the median is used as a measure of central tendency for each category:

$$m_1(x) = median\ of\ all\ gray\ levels\ j\ where: 0 \leq j < x$$

$$m_2(x) = median\ of\ all\ gray\ levels\ j\ where: x \leq j \leq L-1$$

The total mediator is defined as:

$$m_T = median\ of\ all\ gray\ levels\ j\ where: 0 \leq j \leq L-1$$

Where :$m_1(x)$: Median illumination levels, $m_2(x)$: Median illumination levels, m_T :The overall median of all illumination levels in the image.Meanwhile, MAD is used to represent the amount of internal dispersion for the elements of each category as follows[13]

$$MAD_1(x) = median(|j - m_1(x)|) \quad (16)$$

$$MAD_2(x) = median(|j - m_2(x)|) \quad (17)$$

University of Thi-Qar Journal
ISSN (print): 2706- 6908, ISSN (online): 2706-6894
Vol.21 No.2 june 2026

Where: $MAD_1\ (x)$:the median absolute deviation of the first category, $MAD_2\ (x)$:the median absolute deviation of the second category, and then the total internal dispersion is defined as[13]

$$R_w(x) = w_1(x) * [\ MAD_1(x)\ ]^2 + w_2(x) * [\ MAD_2\ (x)\ ]^2 \quad (18)$$

Whereas: $R_w(x)$ Internal dispersion of the hippocampus

The measure of separation between the two groups is expressed based on the differences between the median and the total median:

$$R_b(x) = w_1(x) * [\ m_1(x) - m_T\ ]^2 + w_2(x) * [\ m_2(x) - m_T\ ]^2 \quad (19)$$

Where: $R_b(x)$ The robust variance between the two groups

Therefore, the optimal threshold can be determined by maximizing the proposed robust objective function:

$$J_{ROtsu}(x) = \frac{R_b(x)}{(\ R_w(x) + \varepsilon\ )} \quad (20)$$

Where ε is a very small value to avoid division by zero, and the higher the value of J(x), the greater the statistical separation between the two groups. The optimal threshold is therefore selected as follows:

$$x^* = argmax_x J_{ROtsu}(x) \quad (21)$$

Since x^*: The optimal threshold, the robust ROtsu method provides a segmentation mechanism that is more resistant to noise and outliers than the traditional Otsu method, especially when applied to magnetic resonance images with low contrast and asymmetric distributions.

Steps of the method:

Step 1: Calculate the frequency distribution of the grayscale image

Step 2: Calculate the probabilities of the categories $w_2(x), w_1(x)$ for all threshold values

University of Thi-Qar Journal

ISSN (print): 2706- 6908, ISSN (online): 2706-6894

Vol.21 No.2 june 2026

Step 3: Calculate the median for each category, $m_1(x)$, $m_2(x)$ and the overall median m_T

Step 4: Calculate MAD for each category

Step 5: Calculate ,$R_b(x)$, $R_w(x)$,J_x

Step 6: Select the optimal threshold

Step 7: Convert the image to binary using the selected threshold.

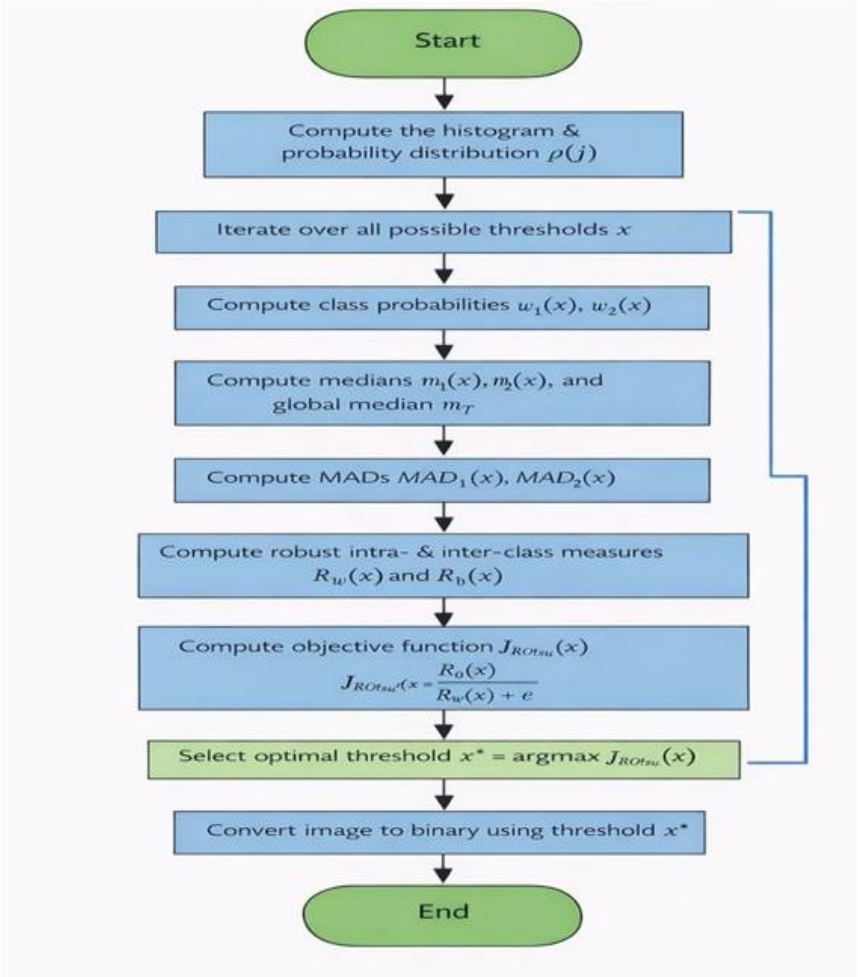

Figure 2.2:shows the flowchart of the Robust Otsu Thresholding method.

2-3.Digital Image Quality Metrics

Digital image quality metrics are used to evaluate how closely a processed image matches the original image and to measure the effect of processing operations such as

noise removal, segmentation, or compression. These metrics are an essential tool for judging the accuracy and efficiency of algorithms used in medical and computer vision applications.

2-3-1.Dice Similarity Coefficient (DSC)

In 1945, Dice introduced a metric for measuring the similarity between two sets, which is widely used in medical image segmentation to measure the overlap between the expected mask and the ground truth. Its value ranges from (0) (no overlap) to (1) (perfect match), and its value increases with increasing segmentation accuracy[19][20].

$$Dice = \frac{|A \cap B|^2}{|A|+|B|} \tag{22}$$

Where: A:the set of predicted pixels for the tumor, B:the set of actual pixels for the tumor, $A \cap B$:correctly predicted pixels (TP),0 ≤Dice≤1

2-10-2.Intersection over Union (IoU) (23)

Jaccard (1912) introduced this index to measure the overlap ratio compared to the union of the two sets. It is a more robust measure in medical images, as it measures the prediction accuracy for both predicted and true regions together[21][22].

$$IoU = \frac{|A \cap B|}{|A \cap B|} \tag{24}$$

It can also be written using TP, FP, and FN values.

$$IoU = \frac{TP}{TP+FP+FN} \tag{25}$$

Be within the scope $0 \leq IoU \leq 1$

2-10-3.Mean Square Error (MSE)

Mean Square Error (MSE) is one of the simplest statistical measures used to evaluate the quality of digital images, as it relies on comparing the pixel values between the filtered image and the original image in terms of luminance. This measure is used to evaluate the amount of change between the pixels of the two images, and its values

University of Thi-Qar Journal
ISSN (print): 2706- 6908, ISSN (online): 2706-6894
Vol.21 No.2 june 2026

range from (0, ∞), where higher values indicate lower image quality. The MSE value is calculated using the following equation[23]:

$$\text{MSE} = \frac{1}{\text{MN}} \sum_{i=1}^{N} \sum_{j=1}^{M} [x(i,j) - y(i,j)]^2 \quad (26)$$

Where:

$x(i,j)$: The pixel value in the original (reference) image at the location (i, j)

$y(i,j)$: The pixel value in the enhanced image at the location (i, j)

MN: The number of elements for which the mean squared error needs to be calculated.

2-10-4.Accuracy: The extent to which the classification of the divided areas[24][25] is correct.

$$\text{Accuracy} = \frac{\text{TP+TN}}{\text{TP+TN+FP+FN}} * 100\% \quad (27)$$

3-Applied aspect

The applied aspect of this research represents a fundamental stage in evaluating the effectiveness of the classical Otsu and robust Otsu methods in segmenting magnetic resonance imaging (MRI) images of brain tumours under the influence of noise. The experiments were conducted using BraTS 2023 (ASNR-MICCAI-BraTS2023-GLI-Challenge-TrainingData) data, which includes mpMRI images of 23 clinical cases collected from multiple medical centres and obtained from the Synapse platform ID: *(syn51156910*). All processing steps and experiments were performed using MATLAB 2024. To study the effect of noise, the original images were used in addition to their corrupted versions, which were produced by adding different levels of Gaussian noise. The classic Otsu and robust Otsu methods were then applied following the same implementation mechanism to ensure fairness of comparison. The segmentation results were compared with the ground truth available in the database. The evaluation was based on quantitative indicators including Dice, IoU (Jaccard), MSE, and Accuracy. The results showed that the robust Otsu method was superior in terms of stability and accuracy in blurred images, achieving higher Dice and IoU values, with a decrease in MSE and an improvement in accuracy compared to the classic Otsu method, indicating

University of Thi-Qar Journal
ISSN (print): 2706- 6908, ISSN (online): 2706-6894
Vol.21 No.2 june 2026

its better ability to reduce the effect of frequency distortion caused by noise. The tables below show the detailed results of the two methods on the original and blurred images.

Table 3.1: shows the results of images according to Otsu's traditional method

Accuracy	IoU	Dice	MSE	ImageName
0.800	0.335	0.502	0.200	1
0.982	0.716	0.835	0.018	2
0.981	0.696	0.821	0.019	3
0.979	0.676	0.807	0.021	4
0.976	0.662	0.796	0.024	5
0.978	0.619	0.765	0.022	6
0.950	0.516	0.681	0.050	7
0.918	0.512	0.677	0.082	8
0.964	0.507	0.673	0.036	9
0.912	0.504	0.670	0.088	10
0.939	0.454	0.625	0.061	11
0.971	0.454	0.625	0.029	12
0.946	0.434	0.605	0.054	13
0.946	0.425	0.597	0.054	14
0.890	0.391	0.563	0.110	15
0.867	0.388	0.559	0.133	16
0.864	0.383	0.554	0.136	17
0.936	0.364	0.533	0.064	18
0.868	0.358	0.528	0.132	19
0.801	0.346	0.515	0.199	20
0.926	0.343	0.511	0.074	21
0.862	0.340	0.508	0.138	22
0.800	0.335	0.502	0.200	23

The results of the Otsu table show that the performance of the method is not consistent across images; some cases (such as images 2–5) achieve relatively good results with Dice values above 0.80 and IoU close to 0.70 when the contrast between the tumor and the background is clear. In contrast, performance in the remaining images drops to Dice values of around 0.50–0.60 with an increase in MSE, indicating poor tumor representation, especially at blurred boundaries or low contrast. Although the apparent accuracy is high (0.86–0.98), it is affected by background dominance and does not reflect the actual segmentation quality. Based on this, the Otsu method shows limited efficiency only in clear cases and remains insufficient for high-accuracy brain tumor segmentation. Figure 3.5 shows an example of the best segmented image.

University of Thi-Qar Journal

ISSN (print): 2706- 6908, ISSN (online): 2706-6894

Vol.21 No.2 june 2026

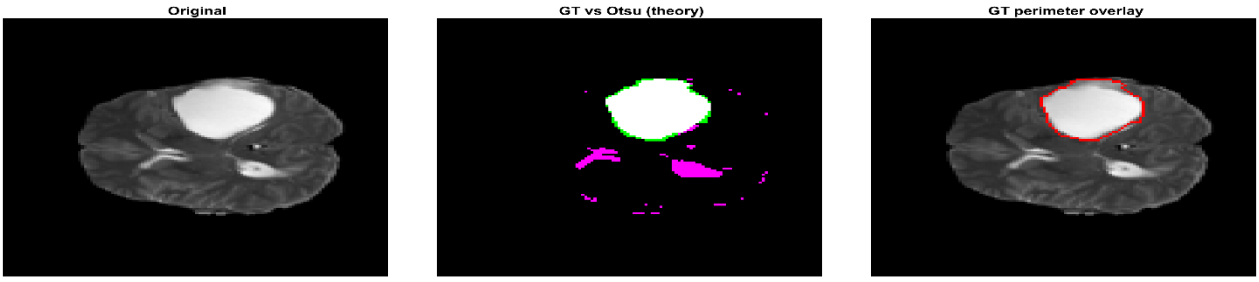

Figure 3.1: shows the division process using the traditional Otsu method

The results show that the Otsu method relies entirely on light intensity, making it sensitive to the similarity of values between the tumor and healthy tissue; therefore, it only succeeds when there is clear contrast and often fails in cases of low contrast. The comparison images (GT vs. Otsu) show frequent classification errors due to similar intensities, with a noticeable deviation in the segmentation boundaries by exceeding healthy areas or neglecting parts of the tumor. These observations confirm that a single threshold is insufficient for complex intensity distribution in MRI images, requiring the use of more advanced methods. The following figures show the metrics used.

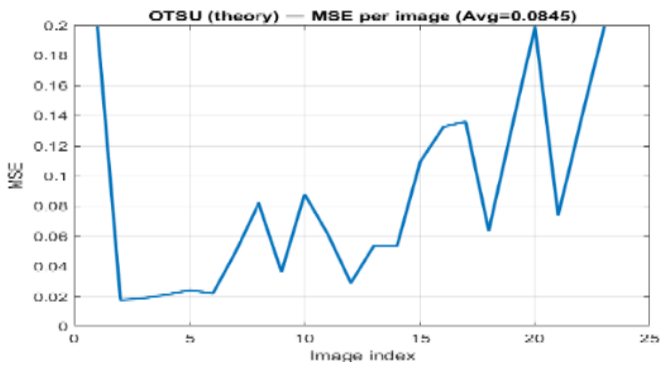

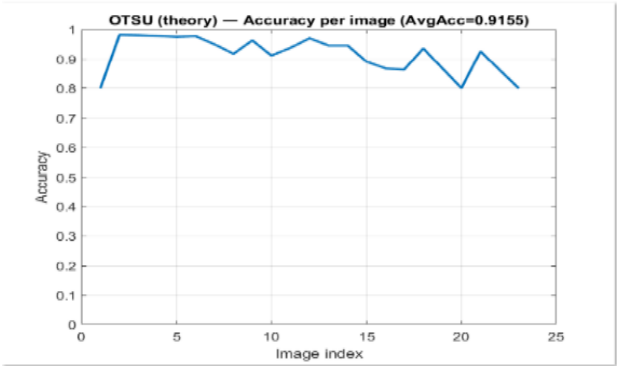

Figure 3.2: shows MSE

Figure 3.3: shows accuracy

University of Thi-Qar Journal

ISSN (print): 2706- 6908, ISSN (online): 2706-6894

Vol.21 No.2 june 2026

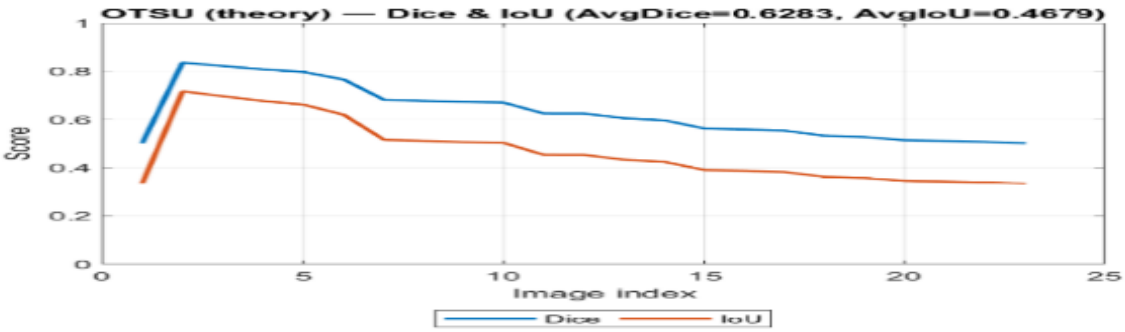

Figure 3.4: shows Dice , IoU

The Otsu method curves under the influence of noise show that accuracy remains relatively high. In contrast, Dice and IoU values gradually decrease with increasing noise, indicating a decline in the ability to distinguish between the tumor and the background. The MSE curve also shows a clear increase when the segmentation deteriorates, confirming Otsu's sensitivity to noise and its unsuitability except at very low noise levels. The table below shows the segmentation of images according to Otsu's method with noise.

Table 3.2: shows the results of images according to Otsu's method with noise

Accuracy	IoU	Dice	MSE	Noise level	ImageName
0.840	0.374	0.545	0.160	0	1
0.828	0.355	0.524	0.172	0.03	1
0.824	0.348	0.517	0.176	0.06	1
0.813	0.329	0.495	0.187	0.1	1
0.826	0.220	0.361	0.174	0	2
0.801	0.199	0.331	0.199	0.03	2
0.792	0.191	0.321	0.208	0.06	2
0.777	0.180	0.306	0.223	0.1	2
0.813	0.215	0.354	0.187	0	3
0.777	0.187	0.315	0.223	0.03	3
0.770	0.182	0.308	0.230	0.06	3
0.767	0.181	0.306	0.233	0.1	3
0.862	0.278	0.435	0.138	0	4
0.828	0.235	0.381	0.172	0.03	4
0.813	0.221	0.362	0.187	0.06	4
0.799	0.208	0.344	0.201	0.1	4
0.836	0.234	0.379	0.164	0	5
0.815	0.213	0.351	0.185	0.03	5
0.815	0.212	0.350	0.185	0.06	5

University of Thi-Qar Journal

ISSN (print): 2706- 6908, ISSN (online): 2706-6894

Vol.21 No.2 june 2026

0.803	0.201	0.334	0.197	0.1	5
0.850	0.219	0.359	0.150	0	6
0.796	0.171	0.292	0.204	0.03	6
0.773	0.156	0.270	0.227	0.06	6
0.780	0.159	0.274	0.220	0.1	6
0.915	0.458	0.629	0.085	0	7
0.833	0.325	0.490	0.167	0.03	7
0.825	0.313	0.477	0.175	0.06	7
0.838	0.323	0.488	0.162	0.1	7
0.849	0.369	0.539	0.151	0	8
0.802	0.311	0.475	0.198	0.03	8
0.790	0.298	0.459	0.210	0.06	8
0.784	0.285	0.443	0.216	0.1	8
0.832	0.206	0.342	0.168	0	9
0.799	0.180	0.305	0.201	0.03	9
0.782	0.166	0.284	0.218	0.06	9
0.776	0.162	0.278	0.224	0.1	9
0.853	0.377	0.547	0.147	0	10
0.836	0.351	0.520	0.164	0.03	10
0.827	0.337	0.505	0.173	0.06	10
0.816	0.321	0.486	0.184	0.1	10
0.816	0.237	0.383	0.184	0	11
0.791	0.216	0.355	0.209	0.03	11
0.783	0.208	0.345	0.217	0.06	11
0.773	0.199	0.332	0.227	0.1	11
0.838	0.172	0.294	0.162	0	12
0.803	0.148	0.259	0.197	0.03	12
0.806	0.150	0.261	0.194	0.06	12
0.799	0.143	0.251	0.201	0.1	12
0.823	0.228	0.371	0.177	0	13
0.783	0.196	0.328	0.217	0.03	13
0.778	0.191	0.321	0.222	0.06	13
0.787	0.196	0.328	0.213	0.1	13
0.818	0.220	0.361	0.182	0	14
0.796	0.202	0.336	0.204	0.03	14
0.789	0.194	0.325	0.211	0.06	14
0.774	0.183	0.309	0.226	0.1	14
0.858	0.321	0.486	0.142	0	15
0.815	0.268	0.423	0.185	0.03	15
0.799	0.254	0.405	0.201	0.06	15
0.807	0.257	0.409	0.193	0.1	15
0.845	0.349	0.517	0.155	0	16
0.820	0.320	0.485	0.180	0.03	16
0.807	0.303	0.465	0.193	0.06	16
0.791	0.284	0.443	0.209	0.1	16
0.867	0.388	0.559	0.133	0	17
0.833	0.336	0.504	0.167	0.03	17
0.825	0.325	0.491	0.175	0.06	17

University of Thi-Qar Journal

ISSN (print): 2706- 6908, ISSN (online): 2706-6894

Vol.21 No.2 june 2026

0.816	0.313	0.477	0.184	0.1	17
0.903	0.307	0.470	0.097	0	18
0.814	0.190	0.319	0.186	0.03	18
0.821	0.195	0.326	0.179	0.06	18
0.818	0.188	0.317	0.182	0.1	18
0.870	0.361	0.530	0.130	0	19
0.835	0.307	0.470	0.165	0.03	19
0.825	0.295	0.456	0.175	0.06	19
0.816	0.283	0.441	0.184	0.1	19
0.809	0.350	0.519	0.191	0	20
0.808	0.348	0.517	0.192	0.03	20
0.805	0.343	0.511	0.195	0.06	20
0.798	0.337	0.504	0.202	0.1	20
0.886	0.260	0.412	0.114	0	21
0.819	0.182	0.308	0.181	0.03	21
0.818	0.180	0.305	0.182	0.06	21
0.815	0.176	0.299	0.185	0.1	21
0.860	0.333	0.499	0.140	0	22
0.812	0.272	0.428	0.188	0.03	22
0.797	0.258	0.410	0.203	0.06	22
0.792	0.249	0.399	0.208	0.1	22
0.840	0.374	0.545	0.160	0	23
0.830	0.358	0.527	0.170	0.03	23
0.825	0.348	0.516	0.175	0.06	23
0.812	0.333	0.500	0.188	0.1	23

Otsu's results under different noise levels show a gradual and clear deterioration in performance; Dice and IoU values decrease with each increase in noise, despite being low in the clean case, confirming the method's high sensitivity to interference. In contrast, MSE increases continuously, reflecting the widening gap between the resulting mask and the true mask, and Accuracy decreases as tumor boundaries become blurred and the contrast on which Otsu mainly relies decreases. Images with relatively good performance in the original case also lose a significant part of their accuracy when noise is added. In general, these behaviors illustrate the limitations of traditional Otsu in dealing with noisy images. Figure 3.9 shows the best divided image model.

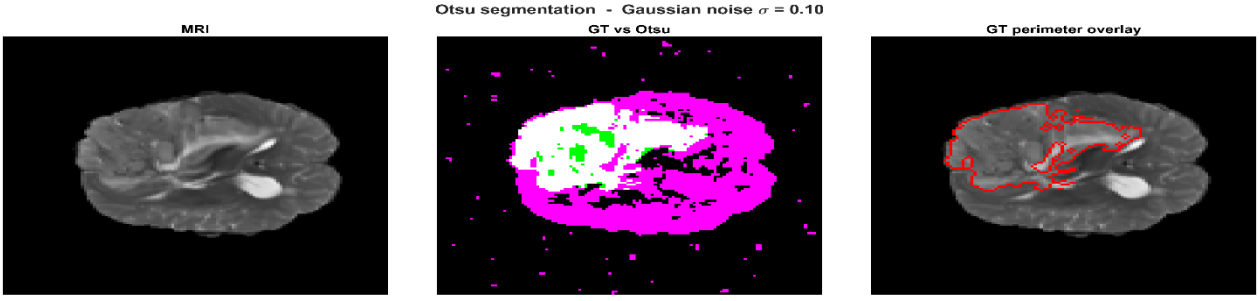

University of Thi-Qar Journal
ISSN (print): 2706- 6908, ISSN (online): 2706-6894
Vol.21 No.2 june 2026

Figure 3.5: shows the segmentation process using Otsu in the presence of noise.

The figures show that the Otsu algorithm is clearly affected by high noise in MRI images; at zero noise, the segmentation is relatively acceptable with marginal errors, while the results gradually deteriorate at levels (0.03, 0.06, 0.1) with an increase in misclassification and distortion of tumor edges. This is due to Otsu's reliance on a fixed threshold that is unable to adapt to noise or intensity heterogeneity, making it unsuitable as a standalone technique for brain tumor segmentation. Table 3.6 shows the image results according to the Robust Otsu method with noise

Table 3.3: shows the image results according to the Robust Otsu method with noise

Accuracy	IoU	Dice	MSE	Noise level	ImageName
0.887	0.380	0.551	0.113	0	1
0.883	0.363	0.532	0.117	0.03	1
0.877	0.338	0.505	0.123	0.06	1
0.874	0.327	0.493	0.126	0.1	1
0.962	0.523	0.687	0.038	0	2
0.945	0.450	0.620	0.055	0.03	2
0.912	0.347	0.515	0.088	0.06	2
0.930	0.364	0.534	0.070	0.1	2
0.977	0.673	0.804	0.023	0	3
0.970	0.581	0.735	0.030	0.03	3
0.952	0.466	0.636	0.048	0.06	3
0.943	0.424	0.595	0.057	0.1	3
0.961	0.553	0.712	0.039	0	4
0.930	0.419	0.590	0.070	0.03	4
0.920	0.380	0.551	0.080	0.06	4
0.920	0.367	0.537	0.080	0.1	4
0.951	0.098	0.179	0.049	0	5
0.962	0.429	0.601	0.038	0.03	5
0.873	0.271	0.426	0.127	0.06	5
0.915	0.325	0.490	0.085	0.1	5
0.968	0.468	0.638	0.032	0	6
0.915	0.311	0.474	0.085	0.03	6
0.917	0.311	0.475	0.083	0.06	6
0.927	0.327	0.492	0.073	0.1	6
0.938	0.413	0.585	0.062	0	7
0.936	0.414	0.586	0.064	0.03	7
0.929	0.389	0.561	0.071	0.06	7
0.928	0.390	0.561	0.072	0.1	7
0.912	0.388	0.559	0.088	0	8
0.896	0.364	0.534	0.104	0.03	8

University of Thi-Qar Journal

ISSN (print): 2706- 6908, ISSN (online): 2706-6894

Vol.21 No.2 june 2026

0.886	0.299	0.460	0.114	0.06	8
0.877	0.286	0.444	0.123	0.1	8
0.913	0.312	0.476	0.087	0	9
0.867	0.232	0.376	0.133	0.03	9
0.869	0.232	0.376	0.131	0.06	9
0.885	0.238	0.384	0.115	0.1	9
0.922	0.410	0.582	0.078	0	10
0.910	0.380	0.551	0.090	0.03	10
0.903	0.359	0.528	0.097	0.06	10
0.901	0.348	0.516	0.099	0.1	10
0.914	0.354	0.522	0.086	0	11
0.907	0.304	0.467	0.093	0.03	11
0.901	0.279	0.437	0.099	0.06	11
0.898	0.283	0.441	0.102	0.1	11
0.967	0.162	0.278	0.033	0	12
0.942	0.345	0.513	0.058	0.03	12
0.876	0.211	0.349	0.124	0.06	12
0.909	0.239	0.385	0.091	0.1	12
0.950	0.289	0.449	0.050	0	13
0.937	0.292	0.452	0.063	0.03	13
0.924	0.281	0.439	0.076	0.06	13
0.908	0.282	0.439	0.092	0.1	13
0.943	0.353	0.522	0.057	0	14
0.936	0.321	0.486	0.064	0.03	14
0.921	0.298	0.459	0.079	0.06	14
0.918	0.278	0.436	0.082	0.1	14
0.936	0.386	0.557	0.064	0	15
0.924	0.344	0.512	0.076	0.03	15
0.918	0.332	0.498	0.082	0.06	15
0.904	0.333	0.499	0.096	0.1	15
0.906	0.403	0.574	0.094	0	16
0.893	0.360	0.529	0.107	0.03	16
0.887	0.326	0.491	0.113	0.06	16
0.890	0.317	0.482	0.110	0.1	16
0.923	0.426	0.597	0.077	0	17
0.912	0.381	0.552	0.088	0.03	17
0.903	0.367	0.537	0.097	0.06	17
0.904	0.352	0.521	0.096	0.1	17
0.947	0.394	0.566	0.053	0	18
0.930	0.343	0.511	0.070	0.03	18
0.921	0.290	0.450	0.079	0.06	18
0.918	0.265	0.418	0.082	0.1	18
0.920	0.416	0.587	0.080	0	19
0.907	0.374	0.545	0.093	0.03	19
0.898	0.337	0.504	0.102	0.06	19
0.898	0.337	0.504	0.102	0.1	19
0.896	0.403	0.575	0.104	0	20
0.895	0.400	0.571	0.105	0.03	20

University of Thi-Qar Journal

ISSN (print): 2706- 6908, ISSN (online): 2706-6894

Vol.21 No.2 june 2026

0.889	0.373	0.544	0.111	0.06	20
0.887	0.350	0.519	0.113	0.1	20
0.952	0.030	0.058	0.048	0	21
0.933	0.336	0.503	0.067	0.03	21
0.905	0.271	0.426	0.095	0.06	21
0.916	0.268	0.423	0.084	0.1	21
0.920	0.423	0.594	0.080	0	22
0.911	0.356	0.525	0.089	0.03	22
0.906	0.330	0.496	0.094	0.06	22
0.913	0.345	0.512	0.087	0.1	22
0.887	0.380	0.551	0.113	0	23
0.879	0.352	0.521	0.121	0.03	23
0.881	0.322	0.487	0.119	0.06	23
0.874	0.333	0.499	0.126	0.1	23

Robust Otsu results under noise show clear superiority over traditional Otsu in terms of stability, achieving higher performance at noise level (0) with Dice values ranging from 0.55 to 0.80, reflecting better ability to handle irregular variation in noisy images. As noise increases, performance gradually decreases, but it remains more stable than the traditional method, with Robust Otsu maintaining acceptable Dice and IoU values at low levels such as (0.03), and Accuracy remaining relatively high in most cases, indicating higher resistance to noise. Although there are some atypical cases (such as images 5 and 21), the general trend confirms that Robust Otsu provides more reliable segmentation in noisy environments. Figure 3.10 shows the best segmented image model.

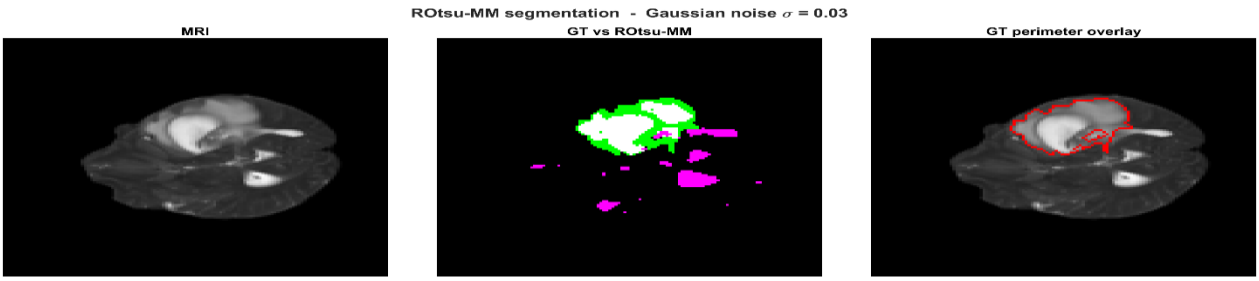

Figure 3.6: shows the segmentation process using robust Otsu.

The figures show that the Robust Otsu method achieves a clear improvement compared to traditional Otsu when isolating tumors under different noise levels, where the separated regions are more coherent with better preservation of tumor boundaries and reduced misclassification. Good agreement with the ground truth is maintained even at

University of Thi-Qar Journal
ISSN (print): 2706- 6908, ISSN (online): 2706-6894
Vol.21 No.2 june 2026

high noise levels, demonstrating the robustness of the method to interference. Overall, the performance shows that Robust Otsu is more stable and efficient than the traditional approach, especially in noisy images. The following figures illustrate the scales used.

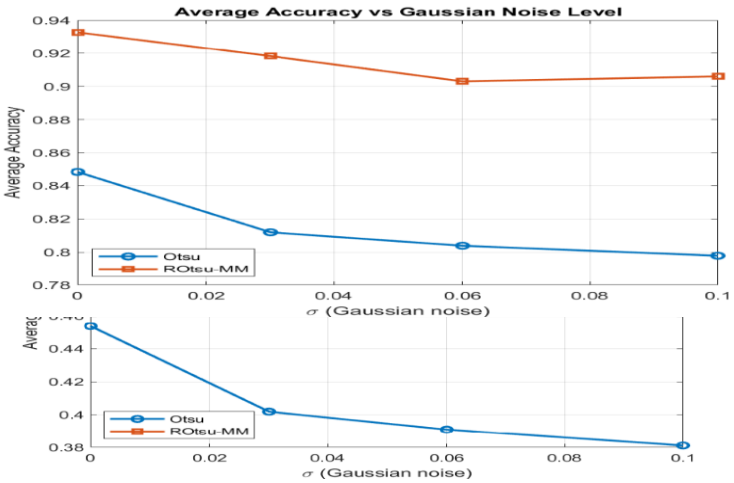

Figure 3.13: shows Accuracy

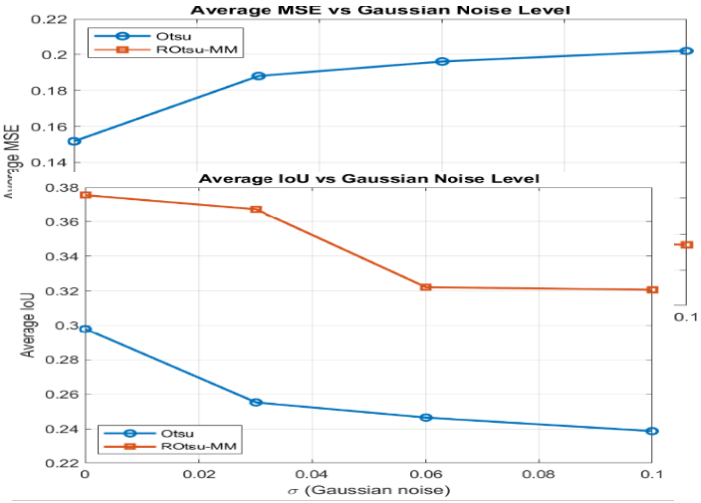

Figure 3.12: shows MSE

Figure 3.11: shows Dice

Figure 3.14: shows IoU

The four curves show the clear effect of noise on the performance of the Otsu and Robust Otsu methods; Otsu's performance deteriorates rapidly with increasing noise, while the proposed method maintains higher and more stable performance. In the MSE curve, Otsu values increase significantly with increasing σ, compared to a slight increase and lower values in Robust Otsu. This is reflected in the Dice and IoU curves, where Otsu's performance decreases sharply at high noise, while the proposed method maintains better overlap with ground truth. Accuracy in Robust Otsu also remains higher than Otsu at all noise levels. Overall, the results confirm that Robust Otsu is more stable and noise-resistant, making it more suitable for segmenting medical images in noisy environments.

Table 3.4: shows the results of the comparison between the methods used in threshold-based segmentation.

Accuracy	IoU	Dice	MSE	Noise level	Method
0.915	0.467	0.628	0.084		Classical Otsu

University of Thi-Qar Journal
ISSN (print): 2706- 6908, ISSN (online): 2706-6894
Vol.21 No.2 june 2026

0.848	0.298	0.454	0.152	0	Otsu with noise
0.933	0.376	0.531	0.067	0	Proposed (with noise)
0.812	0.255	0.402	0.188	0.03	Otsu with noise
0.918	0.367	0.534	0.082	0.03	Proposed (with noise)
0.804	0.247	0.391	0.196	0.06	Otsu with noise
0.903	0.322	0.485	0.097	0.06	Proposed (with noise)
0.798	0.239	0.381	0.202	0.1	Otsu with noise
0.906	0.321	0.484	0.094	0.1	Proposed (with noise)

The comparison table shows that the traditional Otsu method achieves average performance in low-noise images (Dice = 0.628, IoU = 0.467), but deteriorates with increasing noise, with Dice dropping to 0.381 at 0.1 noise, MSE increasing, and Accuracy decreasing, highlighting its sensitivity to noise. In contrast, the proposed method shows more stable performance across all noise levels, with higher Dice values than Otsu, especially at low levels (0.03) where it achieves Dice = 0.534 versus 0.402. The lower MSE and higher Accuracy values also confirm its better ability to reduce false segmentation. Thus, the proposed method is characterized by higher noise resistance and better segmentation quality.

4 -Conclusions

This research presents a comparative study of noise-affected magnetic resonance imaging (MRI) segmentation using the classic Otsu and robust Otsu algorithms. The results show that the performance of the classic Otsu algorithm is clearly affected by the presence of noise due to its sensitivity to frequency distortion, leading to a decrease in the accuracy of separation between the tumour area and the surrounding tissue. In contrast, the robust Otsu algorithm demonstrated remarkable superiority in terms of accuracy and stability, achieving higher Dice and IoU values with a decrease in MSE and an improvement in accuracy. This performance is attributed to the robust version's ability to reduce the impact of noise and outliers on the threshold decision. Therefore, it can be concluded that developing traditional thresholding algorithms to be more robust is a practical and effective solution for improving the segmentation of blurred medical images without the need for high computational complexity.

5 -Recommendations

This research recommends adopting the robust Otsu algorithm instead of the classic Otsu algorithm in medical image segmentation applications, especially in images with noise or low contrast. It is also advisable to expand the scope of experiments to include different databases and imaging devices to verify generalisability and stability. In the future, it is recommended to combine robust Otsu with pre-processing techniques to remove noise or improve contrast, in addition to developing more adaptive versions based on local or multi-level statistical information. The application of this algorithm can also be extended to other noise-affected areas, such as satellite images or industrial images, given its efficiency, simplicity and speed of performance.

References

[1] A. S. Capelle, O. Alata, C. Fernandez, S. Lefevre, and J. C. Ferrie, "Unsupervised segmentation for automatic detection of brain tumors in MRI," *IEEE Int. Conf. Image Process.*, vol. 1, pp. 613–616, 2000, doi: 10.1109/icip.2000.901033.

[2] S. Ruan, D. Bloyet, M. Revenu, W. Dou, and Q. Liaoz, "Fuzzy Random," pp. 237–240.

[3] R. C. Gonzalez and R. E. Woods, "What is Digital Image Processing?," *Digit. Image Process.*, vol. 9, no. 2, pp. 23–25, 2008.

[4] P. Smith, D. B. Reid, C. Environment, L. Palo, P. Alto, and P. L. Smith, "Smith et al. - 1979 - A Tlreshold Selection Method from Gray-Level Histograms," *IEEE Trans. Syst. Man Cybern.*, vol. 20, no. 1, pp. 62–66, 1979.

[5] S. Chen, "Chaotic spread spectrum watermarking for remote sensing images," *J. Electron. Imaging*, vol. 13, no. 1, p. 220, 2004, doi: 10.1117/1.1631316.

[6] P. Buenestado and L. Acho, "Image segmentation based on statistical confidence intervals," *Entropy*, vol. 20, no. 1, 2018, doi: 10.3390/e20010046.

[7] A. G. Jaber, A. M. Eesa, and B. S. Jasim, "Image segmentation by using

thresholding technique in two stages," *Period. Eng. Nat. Sci.*, vol. 9, no. 4, pp. 531–541, 2021.

[8] X. Yan, C. Zheng, Y. Xue, Z. Li, S. Cui, and D. Dai, "Benchmarking the Robustness of LiDAR Semantic Segmentation Models," *Int. J. Comput. Vis.*, vol. 132, no. 7, pp. 2674–2697, 2024, doi: 10.1007/s11263-024-01991-2.

[9] P. S. Liao, T. S. Chen, and P. C. Chung, "A fast algorithm for multilevel thresholding," *J. Inf. Sci. Eng.*, vol. 17, no. 5, pp. 713–727, 2001, doi: 10.1688/JISE.2001.17.5.1.

[10] S. Wang and J. M. Siskind, "Image segmentation with ratio cut," *IEEE Trans. Pattern Anal. Mach. Intell.*, vol. 25, no. 6, pp. 675–690, 2003, doi: 10.1109/TPAMI.2003.1201819.

[11] K. Thapaliya, J. Y. Pyun, C. S. Park, and G. R. Kwon, "Level set method with automatic selective local statistics for brain tumor segmentation in MR images," *Comput. Med. Imaging Graph.*, vol. 37, no. 7–8, pp. 522–537, 2013, doi: 10.1016/j.compmedimag.2013.05.003.

[12] S. J. Nanda, I. Gulati, R. Chauhan, R. Modi, and U. Dhaked, "A K-Means-Galactic Swarm Optimization-Based Clustering Algorithm with Otsu's Entropy for Brain Tumor Detection," *Appl. Artif. Intell.*, vol. 33, no. 2, pp. 152–170, 2019, doi: 10.1080/08839514.2018.1530869.

[13] A. D. V S and S. C. C. S, "Automatic Defect Detection : A Special Case using Titanium Coated Surfaces," vol. 4, no. 17, pp. 1–2, 2016.

[14] J. Wiley, *Robust Statis tics*.

[15] J. H. Xue and D. M. Titterington, "T-Tests, F-Tests and Otsu's methods for image thresholding," *IEEE Trans. Image Process.*, vol. 20, no. 8, pp. 2392–2396, 2011, doi: 10.1109/TIP.2011.2114358.

[16] M. T. N. Truong and S. Kim, "Automatic image thresholding using Otsu's method and entropy weighting scheme for surface defect detection," *Soft*

Comput., vol. 22, no. 13, pp. 4197–4203, 2018, doi: 10.1007/s00500-017-2709-

[17] ROUSSEUW J. and CROUX Christophe, "1993_Alternatives_to_MAD_JASA."

[18] A. Norouzi *et al.*, "Medical image segmentation methods, algorithms, and applications," *IETE Tech. Rev. (Institution Electron. Telecommun. Eng. India)*, vol. 31, no. 3, pp. 199–213, 2014, doi: 10.1080/02564602.2014.906861.

[19] "Gardner - Surg Rounds Orthop - 1990.pdf," vol. 26, no. 3, pp. 297–302, 2012.

[20] A. A. Taha and A. Hanbury, "Metrics for evaluating 3D medical image segmentation: Analysis, selection, and tool," *BMC Med. Imaging*, vol. 15, no. 1, 2015, doi: 10.1186/s12880-015-0068-x.

[21] P. Jaccard, "the Distribution of the Flora in the Alpine Zone.," *New Phytol.*, vol. 11, no. 2, pp. 37–50, 1912, doi: 10.1111/j.1469-8137.1912.tb05611.x.

[22] H. Rezatofighi, N. Tsoi, J. Gwak, A. Sadeghian, I. Reid, and S. Savarese, "Generalized intersection over union: A metric and a loss for bounding box regression," *Proc. IEEE Comput. Soc. Conf. Comput. Vis. Pattern Recognit.*, vol. 2019-June, pp. 658–666, 2019, doi: 10.1109/CVPR.2019.00075.

[23] Hasan Maher Ahmed, "Texture Feature Extraction Using Tamura Descriptors and Scale-Invariant Feature Transform," *J. Educ. Sci.*, vol. 32, no. 4, pp. 91–103, 2023, doi: 10.33899/edusj.2023.143728.1394.

[24] A. Kumar, "Study and analysis of different segmentation methods for brain tumor MRI application," *Multimed. Tools Appl.*, vol. 82, no. 5, pp. 7117–7139, 2023, doi: 10.1007/s11042-022-13636-y.

[25] M. H. Abd al karim and A. A. Karim, "Using Texture Feature in Fruit Classification," *Eng. Technol. J.*, vol. 39, no. 1B, pp. 67–79, 2021, doi: 10.30684/etj.v39i1b.1741.